DEVELOPMENT OF THE LINEAR GRIDLESS ION THRUSTER

Brian E. Beal[*] and Alec D. Gallimore[†]
Plasmadynamics and Electric Propulsion Laboratory
Department of Aerospace Engineering
College of Engineering
The University of Michigan
Ann Arbor, MI 48109 USA

ABSTRACT

The design of the Linear Gridless Ion Thruster, or LGIT, is presented in detail. The LGIT is a hybrid thruster that combines an ionization stage similar to those normally found on gridded ion engines with the acceleration mechanism of a Hall effect thruster. This thruster also features a linear geometry, which simplifies the design of the magnetic circuit while making the LGIT particularly well suited to future work on clustering and, perhaps, thrust vectoring by varying the magnetic fields in the acceleration zone. Initial testing with the thruster operating in a single-stage, unoptimized mode resulted in a specific impulse of 1400 seconds and an anode efficiency of 12%. The low efficiency is believed to be due in large part to operating the thruster in a single-stage mode, rather than the two-stage mode for which it was designed, and to setting the acceleration stage magnets to less than half their design value.

Introduction

The Linear Gridless Ion Thruster, or LGIT, is a two-stage, linear electric propulsion device developed at the University of Michigan[‡]. It is intended to combine the strengths of gridded ion engines with the gridless acceleration mechanism of conventional Hall effect thrusters. The thruster currently being tested is designed for operation in the 2-kilowatt range and has many unique features compared to currently operational plasma thrusters.

In single-stage Hall thrusters, shown schematically in Figure 1, electrons emitted by a downstream hollow cathode backstream toward an upstream anode through an applied magnetic field. As these electrons diffuse back toward the anode, they collide with neutral gas injected at the anode and the propellant is ionized. The magnetic field impedes the motion of the electrons toward the anode and sets up an electric field within an annular discharge chamber.[1] The electric field then serves to accelerate ions toward the exit plane of the thruster. The result is that the same source of electrons is used to both ionize and accelerate a propellant. This affords very little control over the ionization process since it is very strongly coupled to the acceleration process. A result of this coupling is that typical single-stage Hall thrusters have a relatively small operating range over which efficient operation can be maintained.[2] While acceptable efficiency (>50%) has been achieved at specific impulses above 1600 seconds, operation below these values results in rapid declines in thruster efficiency.[2]
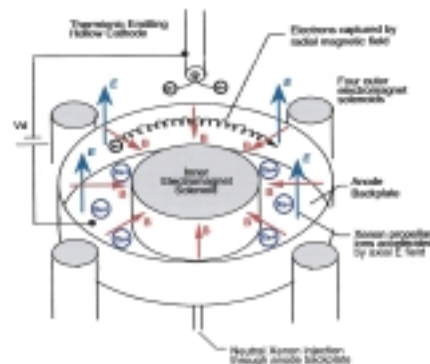

Figure 1: Single-stage Hall thruster. (from Reference 1)

---

* Graduate Student, Student Member AIAA

† Associate Professor, Associate Fellow AIAA

‡ Patent pending

In an effort to gain greater control over the ionization process, two-stage Hall thrusters have been created by introducing an intermediate electrode into the discharge channel. The intermediate electrode then serves as the cathode for the first (ionization) stage and as the anode in the second (acceleration) stage. Figure 2 shows a schematic of a typical two-stage thruster.[3] In some cases, a non-emitting intermediate electrode was used in an attempt to essentially separate the ionization and acceleration zones by controlling the voltage drop in each of the stages.[4] In other cases, an emitting intermediate electrode was used as an electron source for the ionization stage.[5] Both of these approaches have shown promise in increasing total thruster efficiency, which is related to the parameter η in Equation 1, where I represents current, V stands for voltage, and the subscripts 'a' and 'd' denote the acceleration and discharge stages, respectively.[4] As Equation 1 implies, a two-stage thruster's efficiency is maximized by minimizing the power consumed by the ionization, or discharge, process. In practice, this is accomplished by operating the ionization stage at the lowest voltage for which the necessary discharge can be maintained.

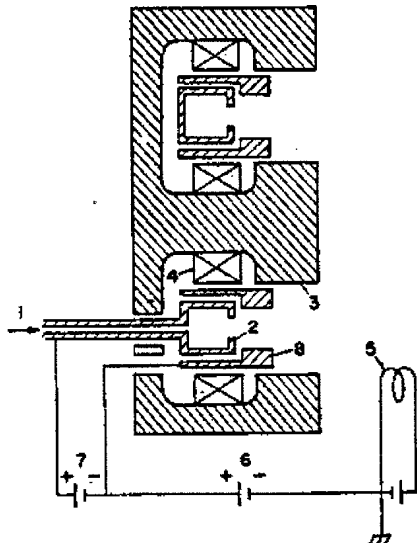$$\eta = \frac{1}{1 + \dfrac{I_d V_d}{I_a V_a}} \qquad (1)$$

Figure 2: A typical two-stage Hall thruster 1) propellant feed, 2) anode, 3) magnetic circuit, 4) magnet winding, 5) cathode, 6) acceleration stage potential, 7) ionization stage potential, 8) intermediate electrode. (from Reference 3)

Design Features

Two-stage Design

The LGIT seeks to improve upon the overall efficiency and throttleability of Hall thrusters by effectively decoupling the ionization and acceleration processes. This is accomplished by using an ionization stage similar to those used in gridded ion engines such as NASA's NSTAR, which uses a ring-cusp magnetic field to enhance ionization. The LGIT ionization stage consists of a hollow cathode surrounded by a rectangular chamber, which serves as the anode. By utilizing two distinct electron sources for the first and second stages, it should be possible to optimize the ionization and acceleration processes nearly independently of each other, thus increasing overall efficiency. Ionization chambers utilizing hollow cathodes and cusped magnetic fields have exhibited ionization costs of approximately 100 W/A in gridded ion thrusters,[6] which is significantly less than the 150-200 W/A normally associated with Hall thrusters.

Ions created in the ionization stage are accelerated through the discharge channel by the electric field created by electrons from the downstream cathode backstreaming toward the anode, just as in a conventional Hall thruster. Using this type of an acceleration mechanism is advantageous because it eliminates the need for grids, the erosion of which constitutes a major failure mode of conventional ion thrusters. Additionally, because the accelerated plasma maintains quasineutrality, space charge limitations are avoided. This allows the LGIT to achieve a much higher thrust density and smaller size than is possible with similarly powered gridded thrusters.

As the previous discussion implies, it is convenient to think of the LGIT as a combination of the ionization stage of a gridded ion thruster combined with the acceleration region of a Hall thruster. The two-stage nature of the LGIT is shown schematically in Figure 3. It should be noted that some of the features shown in Figure 3, such as the size and shape of some components, are exaggerated for clarity.
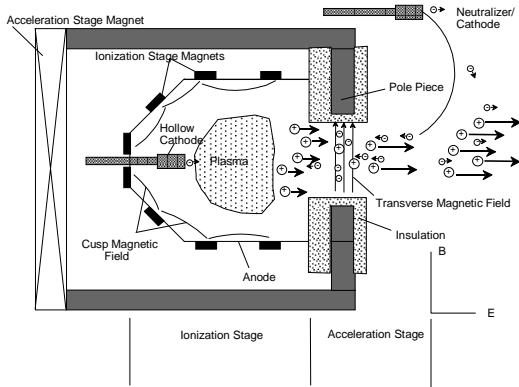
Figure 3: A functional schematic of the Linear Gridless Ion Thruster.

Figure 4: Front view of the linear acceleration stage.

Linear Geometry

One of the most striking features of the Linear Gridless Ion Thruster is its unusual shape. Unlike conventional Hall thrusters that use an annular geometry to facilitate closure of the electron drift current, the LGIT has a linear discharge chamber as shown in Figures 3 and 4. This geometry helped to simplify the development of the magnetic circuit for both the ionization and acceleration stages. Additionally, the linear geometry lends itself to easy spacecraft integration, clustering of multiple thrusters, and possibly to the use of thrust vectoring by varying the magnetic field shape in the acceleration region.

A direct consequence of the linear shape of the acceleration stage is that the Hall current flows across the face of the thruster and is not closed. Researchers at Stanford University have proven that closure of the electron drift current is not necessary by successfully operating a single-stage, linear Hall thruster.[7, 8] To avoid excessive erosion of the ceramic acceleration stage, a tantalum electrode is used to collect the Hall current. There are several options, which will be the subject of future experiments, for handling the current collected by the tantalum electrode. Some of these options include allowing the electrode to float, grounding it, or connecting it to the ionization stage cathode such that the collected current may be re-emitted.
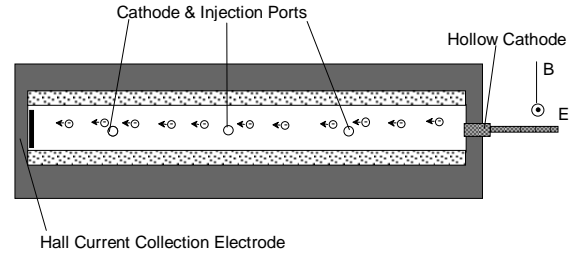
Design Method

Scaling

The thruster being tested was designed for operation at approximately 2 kilowatts. The acceleration stage has been sized to handle a 3 amp discharge at 500 volts with an expected ionization stage power of 500 watts. This assumes ionization costs of approximately 150 W/A.

The overall scaling was accomplished using a combination of empirical scaling laws[9] and by comparison to an existing coaxial thruster.[2] The acceleration channel height and width were determined by scaling from the Air Force/University of Michigan P5 thruster and maintaining a constant current density and aspect ratio. In effect, this dictates that the exit area of the thruster should be proportional to the desired power level for devices operating at comparable voltages. This scaling method was chosen partly to keep the heat transfer to the thruster walls from becoming unmanageable. This method results in an acceleration channel that is 198 mm wide and 22 mm high for a thruster designed to operate at 500 V and 3 A.

The depth of the acceleration channel can be estimated using equations 1.8-1.11 in Reference 3. This calculation results in a suggested channel depth of 18 mm, however this formula is for a stationary plasma thruster (SPT) and hence it assumes that ionization, as well as acceleration, must occur in this depth. Since the plasma is produced in the ionization stage, it was believed that the acceleration stage could be significantly shortened to reduce the loss of ions by recombination at the walls. The actual depth of the acceleration zone was chosen to be 15 mm by optimizing the magnetic field in this region as discussed in subsequent sections of this paper. The acceleration stage is constructed of a

American Institute of Aeronautics and Astronautics

ceramic composed of 50% boron nitride and 50% silicon dioxide.

The height and width of the ionization chamber are sized so that the two stages of the thruster mate smoothly with each other. The rear of the chamber must also be sufficiently large to accommodate a standard NASA 6.4-mm diameter hollow cathode. These considerations led to an ionization stage that is 16 mm high in the back and 22 mm high in the front. The width is 198 mm.

The length of the ionization stage is such that a neutral xenon atom injected at the rear has a high probability of being ionized before escaping into the acceleration zone due to thermal motion. This is accomplished by sizing the discharge chamber such that the characteristic ionization time of an injected xenon atom, τ_{ion}, is significantly shorter than the thermal escape time, τ_{esc}. The escape time is given by Equation 2 and is a function of the length of the chamber (L), Boltzman's constant (k), the temperature of the neutral gas (T_a), and the mass of a xenon atom (m_a). Equation 3 gives the characteristic ionization time, which can be expressed in terms of the xenon number density (n_a) , the electron temperature (T_e), the electron mass (m_e), and the ionization cross section (σ_I).

$$\tau_{esc} = \frac{L}{\sqrt{\frac{8kT_a}{\pi m_a}}} \quad (2)$$

$$\tau_{ion} = \frac{1}{n_a v_e \sigma_i} = \frac{1}{n_a \sqrt{\frac{8kT_e}{\pi m_e}} \sigma_i} \quad (3)$$

In using Equation 3, the temperature dependent ionization cross section, given in m^2 by Equation 4, has been used.[10] Calculation of the ionization time requires an estimate of the neutral xenon density inside the ionization chamber. Since this is difficult to predict analytically, an empirical relation was used. The similarity between the ionization stage of the LGIT and those of gridded ion thrusters makes the use of empirical relations used in ion thrusters appropriate. Equation 5 gives an estimate of xenon number density in m^{-3} based on geometric parameters such as the primary electron area (A_p) and the primary electron volume (Ω_p).[11] The final term involving the

mass and cross sections of xenon and argon is a correction factor to account for the gas being used.

$$\sigma_i = 1.73x10^{-21}T_e(eV) - 2.095x10^{-20} \quad (4)$$

$$n_a \approx 1.4x10^{17} \frac{A_p}{\Omega_p} \frac{\sigma_{Ar}m_{Ar}}{\sigma_{Xe}m_{Xe}} \quad (5)$$

Combining Equations 2-5 and examining a range of expected electron and neutral temperatures led to the selection of a 50 mm long ionization stage. The anode, which is the outer shell of the ionization stage, was constructed of 316 stainless steel. Figure 5 shows a solid model of the ionization stage and ceramic acceleration stage without any of the surrounding components. The stripes on the anode represent the placement of the permanent magnets discussed in the next section (see arrow).
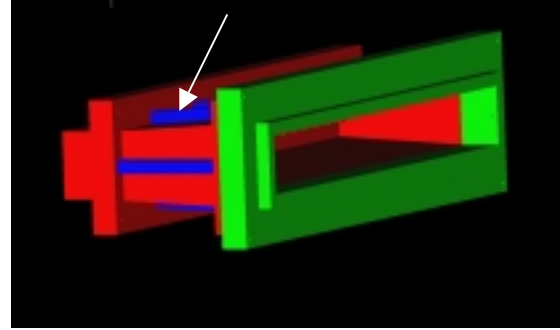

Figure 5: A solid model showing the ionization and acceleration stages without the surrounding components.

Magnetic Circuit

The magnetic field in the LGIT, as in virtually all electrostatic thrusters, is one of the most critical design considerations. As Figure 3 implies, there are two very different magnetic field topologies in the two stages of this thruster. The first stage features cusped fields designed to enhance ionization by increasing the effective path length between the ionization stage cathode and the anode walls. The acceleration stage uses transverse magnetic fields to impede the flow of electrons toward the anode.

The magnetic fields in the acceleration stage have the same function as those in a conventional Hall thruster. The strength of the field is determined by ensuring that the electron

and ion Larmor radii, $r_{l,e}$ and $r_{l,i}$, respectively, satisfy Equation 6, which compares these lengths to the characteristic length of the thruster (L).

$$r_{l,e} << L << r_{l,i} \qquad (6)$$

The magnitude of the magnetic field required in the acceleration zone was estimated by scaling it to the field in the P5 thruster. The goal of the scaling is to keep constant the ratio of the electron gyroradius to the thruster dimensions, $r_{l,e}/L$. This is accomplished by considering the scaling relations used previously where the thruster exit area, and hence the square of the characteristic length scale, was kept proportional to the design power level. Since the electron gyroradius is proportional to the inverse of the magnitude of the magnetic field, it follows that Equation 7 must be satisfied to maintain a constant ratio of gyroradius to characteristic length. In Equation 7, B represents the magnitude of the magnetic field and P represents the nominal thruster power. For a two-stage design, such as the LGIT, the acceleration stage power should be used. Considering that the peak magnetic field strength on the centerline of the 5-kW-class P5 is approximately 250 gauss, Equation 7 suggests a maximum field of 450-500 gauss on the centerline of the LGIT.

$$PB^2 = consant \qquad (7)$$

The ionization stage consists of samarium-cobalt permanent magnets in a cusped configuration to enhance ionization. Both ring-cusp and line-cusp arrangements were considered with an eye toward the ring-cusp option since it has been shown to reduce ionization costs by as much as 20% compared to line-cusp configurations.[6] Unfortunately, it was determined that the ring-cusp design would interfere with the magnetic field in the acceleration region. As shown in Figure 6, a ring-cusp arrangement would have placed magnets having the same orientation next to each other on one edge of the ionization/acceleration interface while placing magnets of opposite orientations next to each other on the other edge. This would have made it impossible to create a symmetric discharge. A line-cusp configuration,

on the other hand, allows the permanent magnets to be arranged in such a way that the magnetic fields are symmetric across both midplanes of the thruster. For this reason, a line-cusp arrangement with the long axis of the magnets running parallel to the flow direction was chosen.
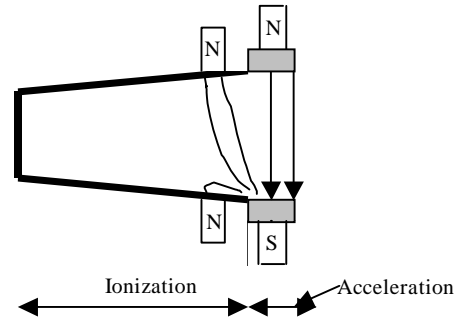

Figure 6: A simplified schematic showing the unacceptable magnetic field interaction that would occur with a ring-cusp design.

After determining the overall magnetic configuration, the 3D magnetic field simulation program MagNet 6.1 was used to size the magnetic pole pieces, determine the screen configuration, and optimize the number and size of permanent magnets used. The main goal of the design was to find an arrangement of permanent magnets that would create a weak field in the middle of the ionization stage to enhance ionization and a strong field near the walls to reduce the loss of primary electrons. This was accomplished by the use of 40 mm long samarium-cobalt magnets with a 5 mm x 5 mm cross section. After an iterative process, a configuration was chosen in which the magnets were arranged with 5 on the top and bottom of the anode and one on each side for a total of 12 magnets. Figure 7 shows the resulting magnetic cusps predicted by the MagNet software. The cross section shown is taken from approximately halfway down the length of the ionization chamber in a direction perpendicular to the flow velocity.
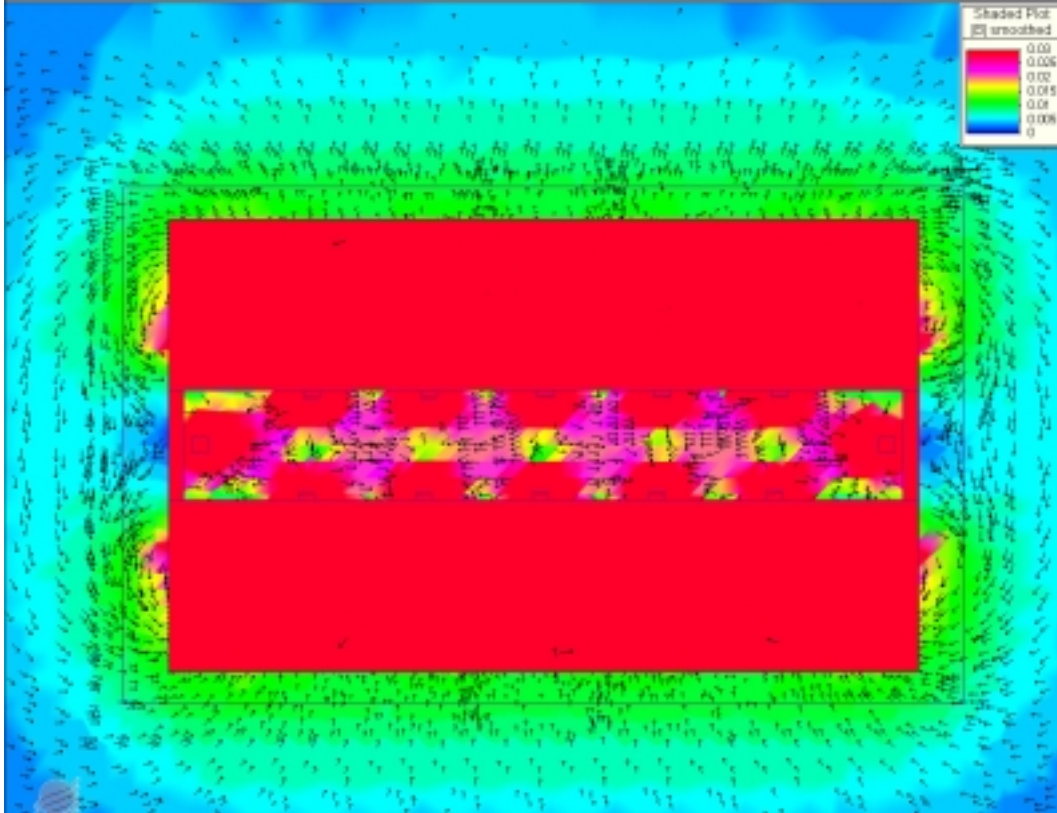
Figure 7: Magnetic cusps predicted by MagNet 6.1 near the midplane of the ionization stage.

An electromagnet circuit constructed of cold-rolled steel provides the transverse magnetic fields in the acceleration region. This circuit was designed to be capable of producing peak magnetic field strengths of at least 750 gauss, well above the expected operating value of 500 gauss. The circuit consists of 8 solid cores connecting 3/8" thick front and back pole pieces. A magnetic screen surrounds the anode to prevent the fields created in the acceleration stage from interfering with the magnetic cusps of the ionization stage. The magnetic circuit, including the rectangular screen, is shown in Figure 8. Figure 9 shows a photograph of the completed thruster.
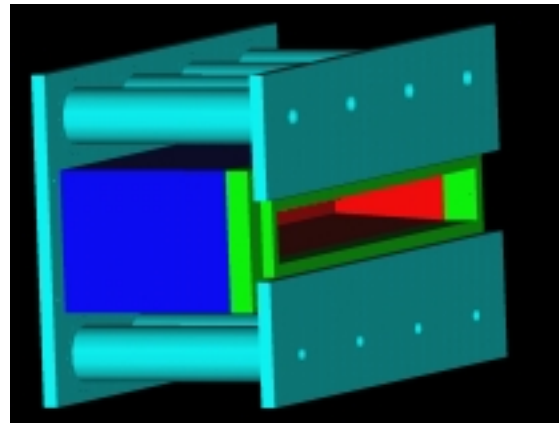

Figure 8: A solid model of the LGIT showing the electromagnet circuit of the acceleration stage.

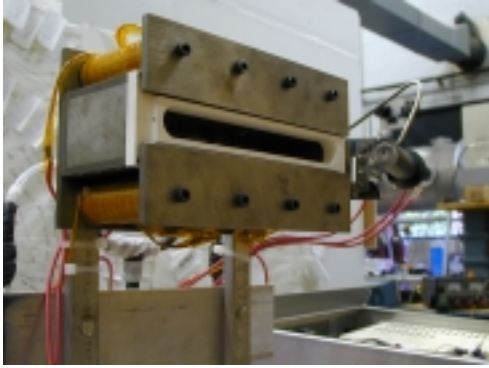American Institute of Aeronautics and Astronautics

Figure 9: The Linear Gridless Ion Thruster.

Recent work has suggested that the shape of the magnetic field in the acceleration zone may affect the loss of ions to the channel walls.[12] There is reason to believe that symmetric, "cupped" magnetic field lines having high strength near the walls and a lower strength near the center of the channel would tend to keep the bulk of the plasma away from the channel walls, thus reducing ion losses due to recombination.[12] In a linear thruster such as the LGIT, symmetric field lines are easy to achieve. As Figure 10 shows, the field lines in the LGIT run nearly perpendicular to the flow direction at the exit plane with cups developing upstream. Figure 10 shows a side view of the thruster. The multiple field lines shown at each axial location represent 5 different streamtraces taken at evenly spaced points across the long dimension (width) of the thruster. It is interesting to note that the lines of force are nearly uniform across the face of the thruster near the exit plane while further upstream the nonuniform field lines are evidence of interaction between the ionization and acceleration stage fields. Figure 11 shows the slightly lower field strength near the center of the

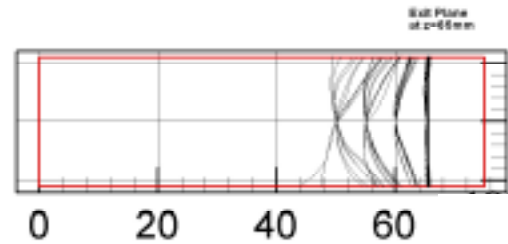acceleration channel compared to near the ceramic walls.

Figure 10: Side view of field lines at 4 different axial locations in the acceleration zone. Note the interaction with the cusp fields evident at the rear of the acceleration stage.

It has been well established that the optimum magnetic field in a conventional Hall thruster consists of a low field strength in the upstream portion of the channel increasing to a peak near the thruster exit plane.[13] As Figure 11 shows, this was achieved in the LGIT by careful placement of the front pole pieces. Note the nearly uniform field strength in the center of the ionization zone and the sharp increase near the exit plane.

Electrical Configuration

The ionization and acceleration stages of the LGIT are powered by Sorensen DCS 55-55 and DCR 600-16T power supplies, respectively. The ionization stage power supply is connected to an isolation transformer to allow it to float at near anode potential. Various laboratory power supplies are used to power the top and bottom electromagnets as well as a heater and igniter for each cathode. A simplified electrical schematic is shown in Figure 12. In Figure 12, the heater, keeper, and electromagnet power supplies are omitted for clarity.
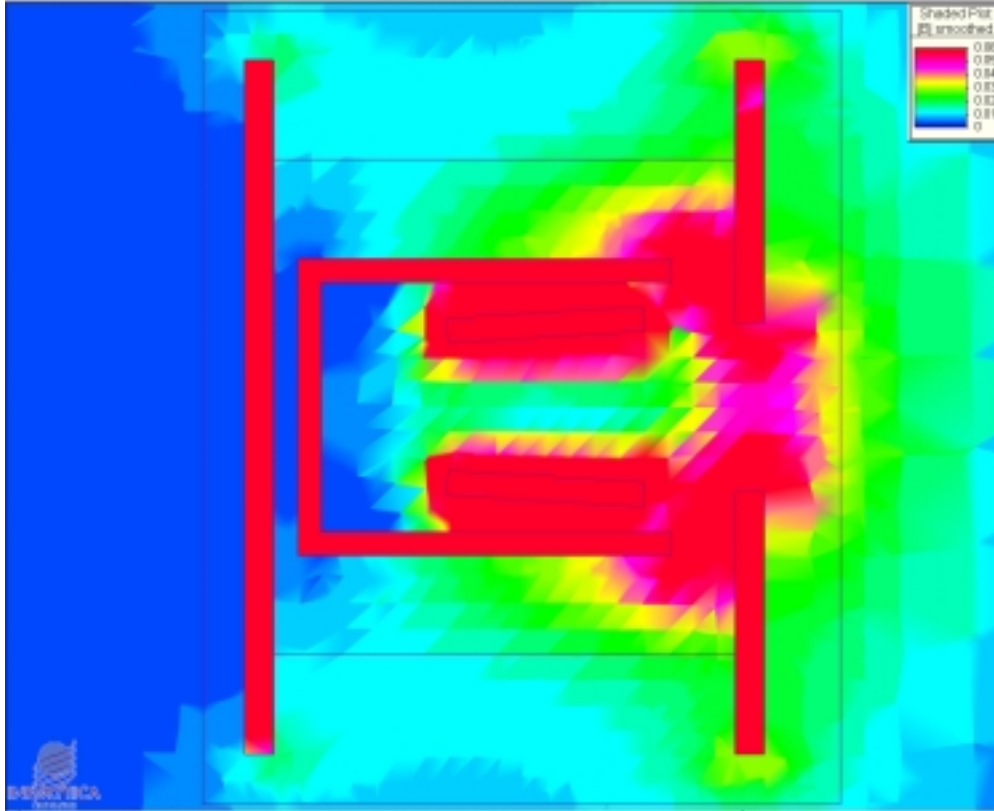
Figure 11: Side view showing the peak in magnetic field strength near the exit plane.
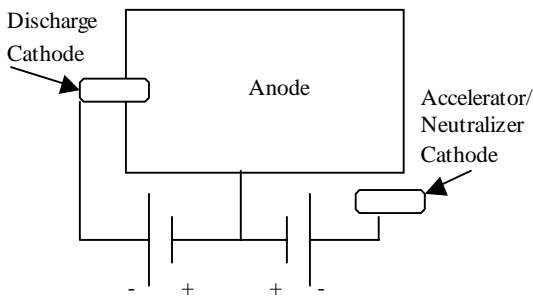

Figure 12: A simplified electrical diagram.

Experimental Setup

Initial tests of the LGIT were conducted in the Large Vacuum Test Facility (LVTF) at the University of Michigan's Plasmadynamics and Electric Propulsion Laboratory (PEPL). The LVTF is a 6-meter diameter by 9-meter long cylindrical, stainless steel vacuum chamber with four large mechanical roughing pumps. Seven nude CVI Model TM-1200 cryopumps provide a pumping speed of approximately 500,000 liters per second on air and 240,000 liters per second on xenon. This facilitates a base pressure of less than 1×10^{-7} Torr and a pressure in the 10^{-6} Torr range during thruster operation. For the initial tests described in this paper, only four of the seven cryopumps were used and the chamber pressure was maintained at less than 1.5×10^{-5} Torr indicated.

The goal of the initial thruster tests was to measure the thrust, specific impulse, and efficiency of the thruster. To accomplish this the LGIT was mounted on a NASA Glenn Research Center type inverted pendulum thrust stand.

Due to difficulties in obtaining a hollow cathode for use in the ionization stage in time to write this paper, initial attempts were made to run the thruster in a single-stage mode. In this mode, the thruster is operated like a conventional Hall thruster, i.e. the ionization stage power supply is completely disconnected. The Hall current collector was electrically grounded.

American Institute of Aeronautics and Astronautics

Experimental Results

The LGIT was initially started in single-stage mode at 300 V with the electromagnets set to approximately half of their design value. The magnets were set to this low value in an attempt to ease thruster startup, with the intent to optimize the magnet settings after a stable discharge was achieved. The anode and accelerator cathode flow rates were set to 15.0 and 6.0 sccm, respectively. The thruster was ignited in this configuration and the resultant discharge current was 3.9 A with the cathode floating at 25.5 V below ground. The thruster maintained a stable discharge for approximately three minutes. Figure 13 shows the LGIT firing for the first time. Unfortunately, before the electromagnet settings were adjusted and optimized, an electrical short between the anode and screen extinguished the discharge.

In the three minutes that the discharge was maintained, the thrust stand recorded a constant thrust of approximately 20 mN. Given the anode flow rate of 15.0 sccm, this constitutes a specific impulse of approximately 1400 seconds. The calculated anode efficiency was 12%. The low efficiency is not surprising considering that the LGIT was operating in a single-stage mode rather than the two-stage mode for which it was designed. Additionally, the discharge current for a mass flow rate of only 15 sccm is expected to be significantly less than the 3.9 A measured. The anomalously high current is most likely the result of the low electromagnet setting. If the magnet settings were to be increased to their design value a significantly lower discharge current is expected.

Figure 13: The LGIT firing for the first time.

Future Work

In the future, the way in which the anode is isolated will be improved upon to prevent the electrical shorts experienced during these techniques. Additionally, a cathode fitting the requirements of the ionization stage will be acquired or built so that the LGIT can be operated in two-stage mode. Once these changes have been implemented, the thruster performance will be measured and optimized at a variety of different power levels. The host of diagnostics available at PEPL will then be used to characterize the thruster both internally and externally.

Acknowledgements

Note to Reader

Many of the figures in this paper were originally created in color and may not be reproduced well here. If the figures are difficult to make out, the reader may wish to view color versions of the figures at the PEPL website: http://www.engin.umich.edu/dept/aero/spacelab/research/publications.

References

1. King, L.B., "Transport Property and Mass Spectral Measurements in the Plasma Exhaust Plume of a Hall-effect Space Propulsion System," Ph.D dissertation, University of Michigan, 1998.
2. Haas, J.M., Gulczinski III, F.S., Gallimore, A.D., Spanjers, G.G., Spores, R.A., "Performance Characteristics of a 5 kw Laboratory Hall Thruster," AIAA 97-3503, 34th Joint Propulsion Conference, Cleveland, OH, July 1998.
3. Kaufman, H.R., "Technology of Closed-Drift Thrusters," AIAA Journal, Vol. 23, No. 1, Jan. 1985, pp. 78-87.
4. Tverdokhlebov, S.O., "Study of Double-Stage Anode Layer Thruster Using Inert Gases,"

IEPC 93-232, 23rd International Electric Propulsion Conference, Seattle, WA, 1993.

5. Yamagiwa, Y., and Kuriki, K., "Performance of Double-Stage-Discharge Hall Ion Thruster," Journal of Propulsion, Vol. 7, No. 1, Jan.-Feb. 1991, pp. 65-70.

6. Sovey, J.S., "Improved Ion Containment Using a Ring-Cusp Ion Thruster," Journal of Spacecraft, Vol. 21, No. 5, Sept.-Oct. 1984, pp. 488-495.

7. Hargus Jr., W.A., and Cappelli, M.A., "Development of a Linear Hall Thruster," AIAA 98-3336, 34th Joint Propulsion Conference, Cleveland, OH, 1998.

8. Schmidt, D.P., Meezan, N.B., Hargus Jr., W.A., and Cappelli, M.A., "Operating Characteristics of a Linear Hall Thruster with an Open Electron-Drift," AIAA 99-2569, 35th Joint Propulsion Conference, Los Angeles, CA, June 1999.

9. Gulczinski, F.S., "Examination of the Structure and Evolution of Ion Energy Properties of a 5 kW Class Laboratory Hall Effect Thruster at Various Operational Conditions," Ph.D dissertation, University of Michigan, 1999.

10. Kaufman, H.R., Robinson, R.S., Operation of Broad Beam Sources, Trade Paperback, 1994, p. 145.

11. Kaufman, H.R., Robinson, R.S., "Ion Source Design for Industrial Applications," AIAA 81-0668R, 15th International Electric Propulsion Conference, Los Angeles, CA 1981.

12. Haas, J.M., "Low-perturbation Interrogation of the Internal and Near-field Plasma Structure of a Hall Thruster Using a High-Speed Probe Positioning System," Ph.D. Dissertation, University of Michigan, 2001.

13. Morozov, A.I., Esipchuk, Y.V., et. al., "Influence of the Magnetic Field Configuration on the Operating Mode of an Accelerator with Closed Electron Drift," Translated from Zhurnal Prikladnoi Mikhaniki I Tekhnicheskoi Fisiki, Vol. 42, 1972, p. 612.